

Climate change impacts on future snow, ice and rain runoff in a Swiss mountain catchment using multi-dataset calibration

Journal Article**Author(s):**

Etter, Raphael; Addor, Nans; Finger, David

Publication date:

2017-10-01

Permanent link:

<https://doi.org/10.3929/ethz-b-000192632>

Rights / license:

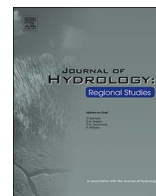
[Creative Commons Attribution-NonCommercial-NoDerivatives 4.0 International](#)

Originally published in:

Journal of Hydrology: Regional Studies 13, <https://doi.org/10.1016/j.ejrh.2017.08.005>

Contents lists available at [ScienceDirect](https://www.sciencedirect.com)

Journal of Hydrology: Regional Studies

journal homepage: www.elsevier.com/locate/ejrh

Climate change impacts on future snow, ice and rain runoff in a Swiss mountain catchment using multi-dataset calibration

Simon Etter^{a,*}, Nans Addor^{a,b}, Matthias Huss^{c,d}, David Finger^e^a Department of Geography, University of Zurich, Winterthurerstrasse 190, CH-8057 Zurich, Switzerland^b Research Applications Laboratory, National Center for Atmospheric Research, Boulder, USA^c Laboratory of Hydraulics, Hydrology and Glaciology (VAW), ETH Zurich, Zurich, Switzerland^d Department of Geosciences, University of Fribourg, Fribourg, Switzerland^e School of Science and Engineering, Reykjavik University, Reykjavik, Iceland

A B S T R A C T

Study region: The hydropower reservoir of Gigerwald is located in the alpine valley Calfeisental in eastern Switzerland. The lake is fed by runoff from rain, snow melt and ice melt from a few small glaciers, as well as by water collected in a neighbouring valley.

Study focus: Water resources in the Alps are projected to undergo substantial changes in the coming decades. It is therefore essential to explore climate change impacts in catchments with hydropower facilities. We present a multi-dataset calibration (MDC) using discharge, snowcover data and glacier mass balances for an ensemble of hydrological simulations performed using the Hydrologiska Byråns Vattenbalansavdelning (HBV)-light model. The objective is to predict the future changes in hydrological processes in the catchment and to assess the benefits of a MDC compared to a traditional calibration to discharge only.

New hydrological insights for the region: We found that the annual runoff dynamics will undergo significant changes with more runoff in winter and less in summer by shifting parts of the summer melt runoff to an earlier peak in spring. We furthermore found that the MDC reduces the uncertainty in the projections of glacial runoff and leads to a different distribution of runoff throughout the year than if calibrated to discharge only. We therefore argue that MDC leads to more consistent model results by representing the runoff generation processes more realistically.

1. Introduction

The Earth's climate is changing. Global surface air temperature is projected to keep rising, while the amounts of snow and ice are declining in all assessed climate scenarios during the 21st century (IPCC, 2014). The impacts on global hydropower potential can hardly be generalized. However, for Europe a loss of about 6% in hydropower potential by 2070 compared to the average potential from 1961 to 1990 is projected (Lehner et al., 2005). It is likely to decrease in all sub-regions except for Scandinavia (Field et al., 2014). For Alpine catchments such as the Rhone basin (Beniston et al., 2014) and several others with hydropower stations (Swiss Society for Hydrology and Limnology (SGHL) and the Swiss Hydrological Commission (CHy), 2011) a slight trend towards decreasing annual runoff is predicted. In Switzerland around 56 % of the electricity production is covered by hydropower (SGHL and CHy, 2011) and is therefore highly dependent on the water availability throughout the year. High-alpine hydropower stations that are snow- and icemelt-dominated will be affected more severely by changing runoff regimes in the next decades (Hänggi et al., 2011; Addor et al.,

* Corresponding author.

E-mail address: simon.etter@geo.uzh.ch (S. Etter).<http://dx.doi.org/10.1016/j.ejrh.2017.08.005>

Received 17 February 2017; Received in revised form 17 August 2017; Accepted 22 August 2017

Available online 12 September 2017

2214-5818/ © 2017 The Authors. Published by Elsevier B.V. This is an open access article under the CC BY-NC-ND license

(<http://creativecommons.org/licenses/by-nc-nd/4.0/>).

2014). This is because a general trend of receding glaciers has been observed since the end of the 19th century according to long-term studies (Bauder et al., 2007; Paul et al., 2007; Zemp et al., 2015). Also the number of days with snowfall decreased from the 1980s until 1999, which is mainly visible at low to mid-elevations (Laternser and Schneebeli, 2003). The days of continuous snow cover as well as the amount of glacier ice acting as natural water reservoirs are projected to decline further or even disappear within the 21st century (CH2014, 2014; Huss et al., 2008). Catchments with a low degree of glacierization will switch from snow-dominated to rain-dominated altering the runoff seasonality towards more winter runoff and less summer runoff. However, the annual runoff is expected to remain at about the same level (CH2014, 2014; Zielr and Bugmann, 2005).

Therefore, annual runoff in glacier-dominated catchments is increasing to a certain maximum and then starts dropping as the glacier surfaces become smaller. The timing of the peak discharge depends on the catchment characteristics and location (Farinotti et al., 2012; Huss et al., 2008). For high-alpine hydropower stations the disappearance of the glacier ice in the long term will most probably lead to a decreasing productivity compared to today (Finger et al., 2012; SGHL and CHy, 2011). Finger et al. (2012) showed that up to one third of the production in the Vispa Valley might be lost due to declining glacier area, projected changes in precipitation and water loss due to inadequate water intakes of the existing hydropower infrastructure by 2100.

Studies for the timing and magnitudes of these discharge alterations can however not be generalized, as suggested by Gaudard et al. (2014) who found also increasing annual runoff sums in the Italian Part of the Alps. They hence have to be performed for every site individually. Nevertheless, possible changes in the seasonal distribution are vital for future water resource management. Even if the effects on the total annual runoff seem to be small, they will have an effect on the water availability for energy production throughout the year. These regime alterations ask for well-balanced management of runoff from Alpine catchments (CH2014, 2014).

Most studies that aim at predicting impacts of climate change use a calibrated hydrological model driven with data of future climate scenarios for projecting discharge until the year 2100. However, the approaches differ in their methodology, the input data and also in their complexity. In recent years the quantile mapping approach developed by Panofsky and Brier (1968) has been increasingly used to correct for systematic biases in climate model outputs, in particular biases in the mean and variability (Teutschbein and Seibert, 2012; Themessl et al., 2011). It has become a standard technique for climate change impact-studies in hydrology (Finger et al., 2012; Ravazzani et al., 2016; Vormoor et al., 2015).

Since the beginning of hydrological modelling research in the 1970s, model calibration focused on fitting simulations to observed discharge data (Boughton, 1966; Johnston and Pilgrim, 1976; Lichty et al., 1968). This practice has also been used in more recent works investigating climate change impacts on water resources in glaciated areas (Köplin et al., 2013; Schaeffli et al., 2007). Since the 1990s, several modelling studies in different fields used additional datasets besides runoff to calibrate hydrological models. Examples are groundwater and soil moisture data (Motovilov et al., 1999), soil saturation (Franks et al., 1998) or stream salinity data (Kuczera and Mroczkowski, 1998). In mountainous regions glacier mass balances and remotely-sensed snow cover proved to be valuable sources of information (Frans et al., 2015; Koboltschnig et al., 2008; Paul et al., 2009). For strongly glacierized catchments, several studies indicated that an accurate modelling of glacier mass balances is crucial (Huss et al., 2008; Magnusson et al., 2010; Stahl et al., 2008). In a catchment with a very low degree of glacierization, however, the role of snow cover becomes more important since it is highly sensitive to changes in temperature as shown by analysing time series of snow records on the West Coast of the United States from 1960 to 2002 (Mote, 2006) as well as by modelling studies in Switzerland (Bavay et al., 2013), Finland (Rasmus et al., 2004) and on a global scale (Barnett et al., 2005). Especially at lower elevations, the snow cover is particularly sensitive to temperature changes (Hantel and Hirtl-Wielke, 2007; Laternser and Schneebeli, 2003). This is one of the main reasons for its important influence on runoff dynamics (Bavay et al., 2013, 2009; Finger et al., 2015; Horton et al., 2006). Finger et al. (2015) showed that if glacier mass balances or snow cover are disregarded in the calibration phase, the model may simulate runoff accurately but for the wrong reasons (Kirchner, 2006) and, hence, lead to a misinterpretation of the components of runoff (rain fall, snow melt, glacier melt). Thus, model results are more likely to be “right for the right reasons” if additional datasets are used for constraining the model. This is particularly important if the model calibration is subsequently used for climate predictions (Finger et al., 2015). The methodology of calibration using multiple datasets and also using quantile mapped climate scenarios has only been applied using the physically based TOPKAPI model (Finger et al., 2012). With a transfer of the methodology to a conceptual model, such as the Hydrologiska Byråns Vattenbalansavdelning (HBV)-light model (Seibert and Vis, 2012) the calculations could be done more efficiently permitting to explore the entire parameter space.

The objectives of this paper are (i) to demonstrate that the multi-dataset calibration (MDC) leads to more realistic hydrological simulations under present climate, and hence, to more reliable projected changes, than a calibration based on discharge alone Q_{only} ; (ii) to quantify the contribution of the different components of the model chain to the uncertainty in projected discharge using an analysis of variance (ANOVA); and (iii) to assess the impacts of climate change on glaciers, snow and runoff in the catchment of the Gigerwaldsee with the MDC in comparison to Q_{only} . These objectives provide the structural sub-headings used in the Methods, Results and Discussions sections, namely: (i) Multi-Dataset Calibration, (ii) ANOVA, and (iii) Discharge Scenarios.

2. Study site and data

2.1. Study site

The Gigerwaldsee lies in eastern Switzerland, about 80 km southeast of Zurich (see Fig. 1). The lake has a usable volume of $33.4 \times 10^6 \text{ m}^3$ and a surface area of 0.71 km^2 . It is fed by its natural catchment, the Calfeisental (52 km^2) and also by eight partial catchments with a total area of 45 km^2 , where water is collected from the Weisstannental (see numbers 1–7 in Fig. 1) in the North and the small Tersoltal (8) in the East of the Calfeisental. Electricity is generated in the power plant Mapragg the compensating reservoir

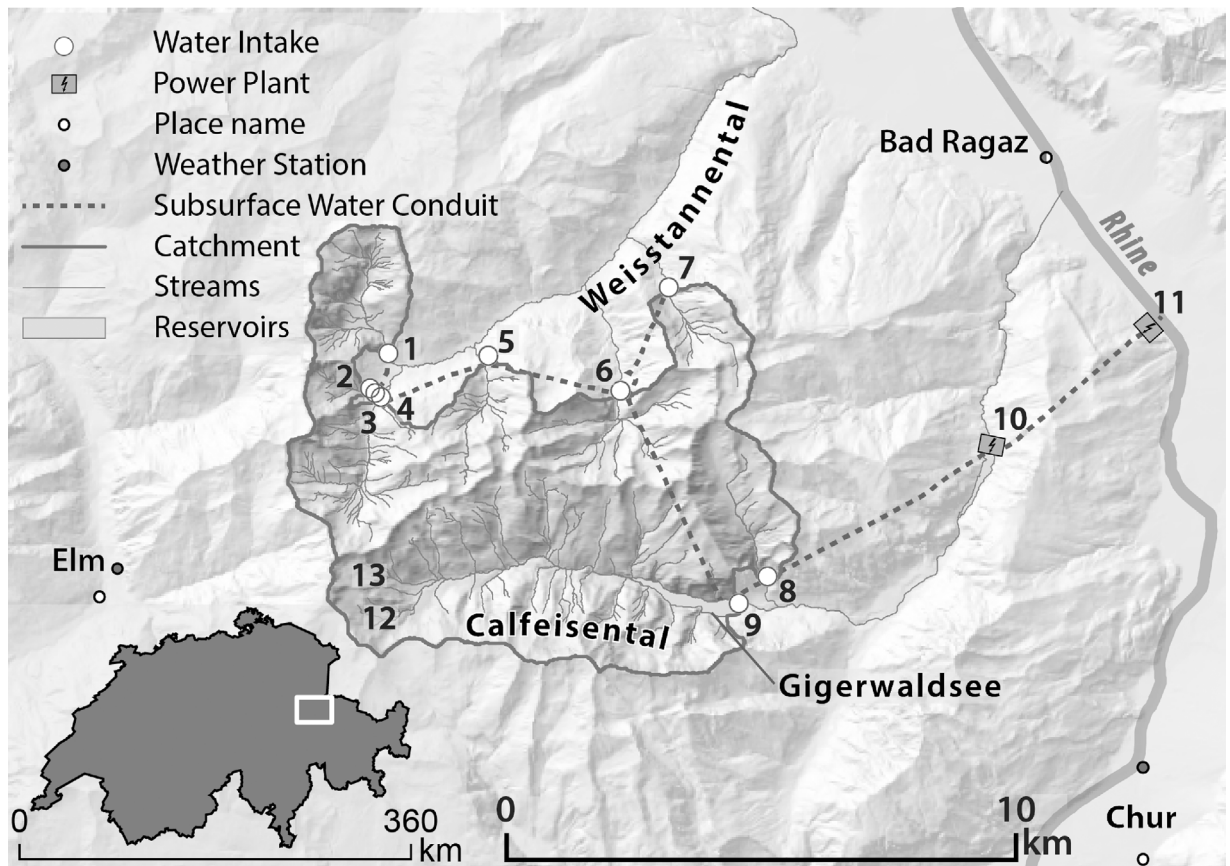


Fig. 1. Overview of the watershed of Gigerwaldsee. See text for explanations of numbers.

Mapraggsee (10) and in the valley bottom in Sarelli (11). The three biggest glaciers, but still small in size, are the Sardonagletscher (12) with an area of 0.45 km² the Chline Gletscher (13) with 0.21 km² and the Pizolgletscher (14) with 0.09 km². The glacier areas refer to the year 2008 (Fischer et al., 2014) and cover an area of less than 1 % of the entire study area. Ringelspitz is the highest point of the catchment with 3247 m a.s.l. This catchment was chosen since it offers interesting features like snow and glacier areas, as well as the anthropogenic connections to the neighbouring valley. The representation of these features could therefore be tested in the model.

2.2. Data

The discharge data was provided by the Kraftwerke Sarganserland AG and is computed using the water balance of the reservoir. Hence, the inflow to the lake was calculated from the change of the water content in the lake, the water used for power production and the evaporation and is available from August 1997–December 2011. Discharge was provided as daily values divided into the discharges from the Calfeisental and the Weisstannental.

The climate data for the past were obtained from MeteoSwiss and consist of interpolated station measurements of temperature (Frei, 2014) and precipitation (Frei et al., 2006; Frei and Schär, 1998; Schwarb, 2000). The datasets for daily mean temperature and daily precipitation have a resolution of 2.2 km, although the spacing between the measurement stations is larger.

Fractions of snow-covered area of the catchment were obtained from the MOD10A1.5-product with a resolution of 500 × 500 m of the years 2001–2008. This was in turn acquired by the space-borne moderate resolution imaging spectroradiometer (MODIS), which is orbiting the earth since 2001 on the Terra satellite (Hall et al., 2002).

Outlines for all glaciers in the catchment are available for 1973 and 2008 based on glacier inventory data (Fischer et al., 2014). Annual mass balances for each individual glacier in the Gigerwaldsee catchment were derived by combining thickness changes between 1980 and 2008 obtained from two digital elevation models (DEMs) with data of year-to-year variability (Fischer et al., 2015). Ice thickness distribution on a regular 25 × 25 m grid was calculated based on Huss and Farinotti (2012). Results were validated against measurements of ice thickness on Sardonagletscher and Pizolgletscher acquired in 2010, and direct measurements of seasonal glacier mass balance of Pizolgletscher since 2006 (Huss, 2010; Huss and Fischer, 2016).

Future climate scenarios were needed in order to calculate the discharge scenarios. They were obtained from the ENSEMBLES project (van der Linden and Mitchell, 2009). Seven combinations of global circulation models (GCM) and regional climate models (RCM) based on the A1B emission scenario were chosen (see Table 2).

When this study was started in 2014, we decided to use RCM projections from the ENSEMBLES project, which rely on GCM runs from the third phase of the Coupled Model Intercomparison Project (CMIP3). RCM projections driven by the following GCM generation (CMIP5) have now been produced in the framework of the EURO-CORDEX project, but when this study was initiated, only few EURO-CORDEX runs were available. To sample the climate model space, we preferred using a large number of models from the ENSEMBLES generation, than a small sample of models from the newest EURO-CORDEX generation, as this might have led to an underestimation of the climate model uncertainty (Knutti et al., 2013). Further, evaluation of the EURO-CORDEX models revealed that some of them unrealistically accumulate snow in the Alps (Terzago et al., 2017). We consider this to be a major issue for our study in a snow-dominated mountainous basin.

3. Methods

3.1. Multi-dataset calibration

3.1.1. Model setup

The HBV-light model is a semi-distributed model (Seibert and Vis, 2012), which means that the entire drainage area, including intakes from subsidiary watersheds, is represented by elevation bands based on a local DEM. Therefore, all the subcatchments, where the water intakes are located, and the natural watershed of the Gigerwaldsee are summed up into one catchment (Fig. 1).

Further, hydrological response units (HRUs) were defined. Since a higher specification of vegetation zones does not necessarily lead to better simulation results (Finger et al., 2015), only two land cover types are considered and the catchment was divided into glacierized and non-glacierized areas. This was confirmed by the results of some preliminary test runs with three vegetation zones including forest and open soils or grass land, where the discharge representation did not improve when using more HRUs. The HRUs were represented in fractions of total catchment area per (200 m) elevation and aspect zone (North, South and East/West).

The temperature (in °C) and the precipitation (mm/day) were averaged over the entire catchment. Inside the model they were then adapted for each elevation zone using calibrated factors. Potential evapotranspiration (PET) was calculated depending on temperature and the latitude of the weather station using the method developed by McGuinness and Bordne (1972). Temperature based methods tend to overestimate evapotranspiration with increasing temperatures (Sheffield et al., 2012) and more physically based methods might provide more accurate estimations of PET. But as the terrain in this study is very complex, data requirements for more complex approaches are very hard to fulfil (e.g. no local measurements on wind speed are available). Furthermore, wind speeds for the future are only available on a 25 km grid in the RCM outputs, of which the reliability is highly doubted for the Alpine region (Tobin et al., 2015). We therefore decided to stick to the temperature based approach, being aware of its limitations.

3.1.2. Glacier routine

The HBV-light model (Seibert and Vis, 2012) has recently been modified with a dynamically adapting glacier routine based on the Δh -parameterization in Huss et al. (2010). The same parameterization was recently also implemented in a distributed version of the HBV model (Beldring et al., 2003) and was tested in three high mountain areas. It performed well as long as the input data was of sufficient quality (Li et al., 2015). The parameterization in the present model calculates not only the discharge and the snow-covered fraction of the catchment area, but also dynamically simulates the present glacier water equivalent per elevation area over the simulation time. The model is thus able to simulate glacier retreat and advance. The new glacier routine is described in Seibert et al. (2017).

3.1.3. Model calibration

In order to calibrate the HBV-light model, we performed 10,000 Monte Carlo (Metropolis and Ulam, 1949) simulation runs to identify suitable parameter sets using uniformly distributed parameter values (Beven and Binley, 1992; Uhlenbrook and Sieber, 2005), similarly to Finger et al. (2011). The scores of the 10,000 parameter sets were then calculated according to the objective functions listed below:

The performance metric most commonly used for conceptual hydrological models is the Nash-Sutcliffe efficiency (Nash and Sutcliffe, 1970). It compares the observed discharge value (Q_{obs}) to the simulated discharge (Q_{sim}) at each time step i :

$$NSE = 1 - \frac{\sum_{i=1}^n (Q_{i,obs} - Q_{i,sim})^2}{\sum_{i=1}^n (Q_{i,obs} - \overline{Q_{obs}})^2} \quad (1)$$

To give more weight to the low-flow season, we also used the logarithmic Nash-Sutcliffe efficiency:

$$\logNSE = 1 - \frac{\sum_{i=1}^n (\log(Q_{i,obs}) - \log(Q_{i,sim}))^2}{\sum_{i=1}^n (\log(Q_{i,obs}) - \log(\overline{Q_{obs}}))^2} \quad (2)$$

To evaluate the performance of the snow cover simulation, we used the correctly predicted snow covered area (CPSC) – a metric based on the snow-covered area fraction of the catchment introduced in Finger et al. (2015) for the semi-distributed HBV-light model structure. The absolute difference between the simulation and the observation is subtracted from 1, then summed up for every time step and finally averaged. If the result is equal to 1, the snow cover is predicted perfectly.

$$CPSC_A = \frac{1}{n} \sum_{i=1}^n (1 - |a_{i,obs} - a_{i,sim}|) \quad (4)$$

The CPSC-metric was calculated for summer only, from April 1st to August 31st, (CSPC_s) and over the whole year (CSPC_y). a_i represents the snow covered area fraction of the observations and the simulations. The glacier mass balance simulation could only be evaluated once a year on October 1st, since the data was only available on that day. However, the root-mean square deviation was calculated for each of the four years of the simulation.

$$MB_{RMSD} = \sqrt{\frac{1}{m} \sum_{i=1}^m (B_{i,ref} - B_{i,sim})^2} \quad (5)$$

B is the glacier mass balance, expressed in mm of water equivalent, n is the number of points during the observed period. To obtain a weighted average of all performance measures we used the normalized overall efficiency performance index P^{OAnorm} that was introduced in Finger et al. (2011) to produce climate change projections in Finger et al. (2012), and to test performance in different model complexities in Finger et al. (2015). Accordingly, here we only provide a short summary and refer to the original literature for a more detailed description. First, the average of the rank for every parameter set regarding the efficiency criteria for discharge (Q), snow cover (SC) and glacier mass balances (MB) is calculated. The average ranks are then normalized by dividing the average rank by the highest average rank of all MC runs resulting in an overall efficiency performance, P^{OAnorm} , ranging between 0 and 1, with 1 indicating the best possible performance.

The calibration of the model was performed for the years 2001–2004 and the validation in the period 2005–2008. During these two periods the discharge, snow cover and glacier mass balance data was fully available.

3.1.4. Parameter ensembles selection

From the 10,000 Monte Carlo runs the parameter sets were ranked according to their performance in the P^{OAnorm} . The ten best sets were considered to be equifinal. The parameter ranges and the selection of parameters to be calibrated (Table 1) were derived from previous studies and experience using HBV (Finger et al., 2015; Geris et al., 2015). To assess the benefit of using multiple datasets and objective functions to calibrate the model, several combinations of objective functions were evaluated. The model was calibrated to

Table 1
Overview of the calibrated model parameters of the HBV model.

Parameter	Description ^a	Unit	Min	Max	Mean(10)	Std(10)
Rescaling Parameters of Input Data						
PCALT	Change of Precipitation with elevation	% (100 m) ⁻¹	1	20	9.80	5.97
TCALT	Change of temperature with elevation	°C (100 m) ⁻¹	0.1	1	0.49	0.13
Snow and ice melt parameters						
TT	Threshold temperature for liquid and solid precipitation	°C	-2	0.5	-0.76/-0.93	0.82/0.70
CFMAX	Degree-day factor	mm d ⁻¹ °C ⁻¹	0.5	10	7.18/3.01	1.99/1.03
SFCF	Snowfall correction factor	-	0.5	0.9	0.76/0.68	0.10/0.09
CFGlacier	Glacier melt correction factor	-	0.1 (1 where no glacier)	5 (1 where no glacier)	1/1.22	0/1.15
CFSlope ^b	Slope snow melt correction factor	-	1	5	1.87/2.70	0.44/1.12
KGmin ^c	Minimum value for the outflow coefficient representing conditions with poorly developed glacial drainage system in late winter	-	0.01	0.2	0.11	0.06
dKG ^c	Range of the annual outflow coefficient variation	-	0.01	0.5	0.21	0.13
AG ^c	Calibration parameter defining the sensitivity of the outflow coefficient to changes in the snow storage	-	0	10	5.79	2.73
Soil Parameters						
PERC	Maximum percolation from upper to lower groundwater storage	mm d ⁻¹	0	4	1.88	1.09
K0	Storage (or recession) coefficient 0	d ⁻¹	0.1	0.5	0.29	0.13
K1	Storage (or recession) coefficient 1	d ⁻¹	0.01	0.2	0.12	0.04
K2	Storage (or recession) coefficient 2	d ⁻¹	5E-05	0.1	0.04	0.02
MAXBAS	Length of triangular weighting function	D	1	6	2.75	1.44
FC	Maximum soil moisture storage	mm	100	550	372.52/297.19	121.36/140.24
LP	soil moisture value above which actual evapotranspiration reaches potential evapotranspiration	-	0.3	1	0.61/0.65	0.212673/0.22
Beta	Shape factor for the function used to calculate the distribution of rain and snow melt going to runoff and soil box, respectively	-	1	5	2.90/3.36	1.367984/1.22

^a A detailed description of model parameters is given in Seibert and Vis (2012).

^b Slope factor correcting CFMAX accounting for dependency of melt rates on aspect of topography.

^c Glacier parameters according to Stahl et al. (2008).

Table 2

Comparison of the seven corrected climate models compared to observed climate used for the bias correction in the period 1980–2009. The values are quantile-mapped (see Section 3.3.1). MD represents the mean difference of each day of the scenario and the corresponding observations. R is the ratio of the standard deviations of the simulated and the observed period during the period 1961–2011. P and T stand for precipitation and temperature respectively.

No.	Global CM	Institute	Regional CM	MD _T (°C)	MD _P (mmd ⁻¹)	R _T (–)	R _P (–)
1	ARPEGE	CNRM	ALADIN5.1	0.001	0.015	1.006	1.033
2	ARPEGE	DMI	HIRHAM5	0.001	–0.001	1.021	1.020
3	HadCM3Q0	ETHZ	CLM	–0.013	–0.004	1.021	1.038
4	HadCM3Q0	HC	HadRM3Q0	–0.006	0.013	1.027	1.021
5	ECHAM5-r3	KNMI	RACMO2	0.000	0.023	0.993	1.052
6	ECHAM5-r3	MPI	REMO	–0.000	0.005	0.996	1.051
7	BMC	SMHI	RCA	–0.001	0.006	1.001	1.039

Q, using Nash-Sutcliffe and logarithmic Nash-Sutcliffe efficiency, SC, using the correctly predicted snow-covered area over summer and also for the entire year and finally MB using the root-mean square error. The calibration was performed to Q, SC and MB only, all possible combinations of two of these and all three criteria combined. Then, the ten best sets were selected using P^{OAnorm} . The purpose and advantage of the MDC method is to move away from calibrating using solely discharge data, and instead, to account simultaneously for different observational datasets by giving them the same weight. This may lead to slightly lower NSE values than when Q is the only dataset used for model calibration, but previous studies showed that it results in more realistic simulations (see Finger et al., 2015, 2012, 2011). Furthermore, in test runs MDC revealed to generate more realistic mean values regarding the temperature lapse rate (Table 1).

Additionally, we compared the resulting hydrographs for the calibration and validation periods of the Q_{only} calibrations with the results of the MDC. Thereby we can evaluate the benefits of the MDC for the simulation of the individual runoff components.

3.2. ANOVA

An analysis of variance (ANOVA) was used in order to assess the total uncertainty of the MDC-driven discharge simulations in Section 3.3. In this modelling chain, variations from all the used datasets contribute to the uncertainty in the result. Therefore a procedure similar to previous works (Addor et al., 2014; Bosshard et al., 2013; Finger et al., 2012) is applied: A three-way analysis of variance (ANOVA) for the period 2036 to 2065 and a two-way ANOVA for the period from 2069–2098 are conducted. For the later period a two-way ANOVA is used, because the glaciers are predicted to have disappeared by the start of that period. The objective was an analysis of the contributors to the global uncertainty, i.e. the relative contribution to the variance of the simulated discharge of the three effects. Those are the seven climate scenarios, three glacier scenarios and the ten parameter sets. According to the theory of ANOVA (von Storch and Zwiers, 1999) the sum of squares of the different independent variables and the sum of squares of their interactions sum up to the sum of squares of the total.

3.3. Discharge scenarios

The third objective of this work is to produce estimates of the climate change impacts on the runoff in the watershed of the Gigerwaldsee and to show the difference in the results of a calibration using a MDC compared to the calibration to discharge only. To that end, the model was driven by GCM-RCM simulations using once the ten best parameter sets that were found using all available datasets and once using discharge only for calibration.

3.3.1. Bias-correction of climate projections

Significant differences may exist between local weather observations and GCM-RCM simulations under current climatic conditions. They are usually referred to as ‘model biases’ (Christensen et al., 2008) but can also emerge from natural variability and interpolation errors (Addor and Fischer, 2015). These differences can impede the performance of hydrological models (Muerth et al., 2013). Hence, in order to be able to use climate simulations for impacts studies, various bias-correction methods have been developed. A method delivering particularly satisfactory results, while being straightforward to be implemented and run, is quantile mapping (Panofsky and Brier, 1968; Themessl et al., 2011). This implies the transformation of a climate simulation so that its cumulative distribution function after the transformation corresponds to that of the observations (Piani et al., 2010). The method is calibrated over a 30-year reference period and is then applied to future conditions, i.e., a key assumption is that the biases are stable over time. For this study, we used the variant of quantile mapping relying on empirical quantiles (Gudmundsson et al., 2012) and applied it to the seven ENSEMBLE models outlined in Table 2. The reference datasets for temperature and precipitation are again the gridded daily temperature and precipitation datasets called TabsD (Frei, 2014) and RhiresD (Frei et al., 2006; Frei and Schär, 1998; Schwab, 2000), respectively. Quantile mapping shows limitations when multi-day statistics are scrutinized (Addor and Seibert, 2014), but this is not of great concern in this study, which focuses on changes in the annual cycle averaged over 30 years.

3.3.2. Glacier scenarios

To minimize the errors in glacier evolution due to the coarse resolution of the HBV- light model and the small glacier size, we used

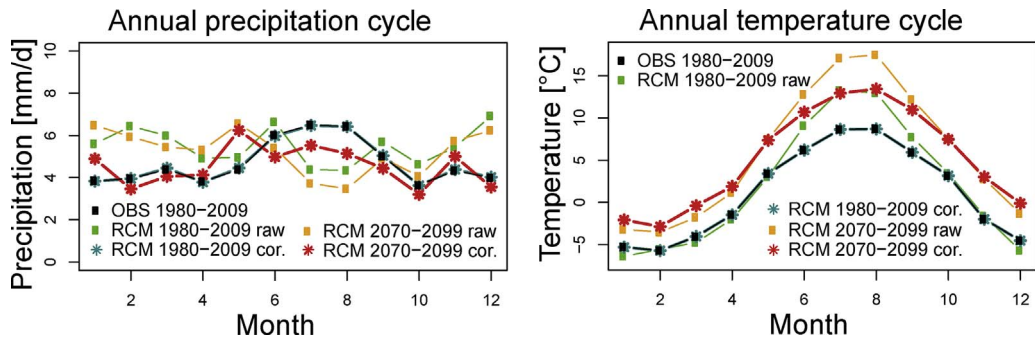


Fig. 2. Quantile-mapping corrected precipitation and temperature values of an example GCM (HadCM3Q0) RCM (ETHZ-CLM) scenario.

the spatially distributed glaciological model GERM (Huss et al., 2008) to calculate spatial glacier extents for the three considered time periods in the 21st century. Therefore, the HBV runs for modelling discharge scenarios were re-initiated with the newly modelled glacier areas from GERM for the two future periods.

By combining the new parameter sets with climate and glacier scenario data, discharge scenarios for the catchment were calculated. The runoff was simulated for a baseline period from 1992 to 2021 and two future periods for the middle of the century from 2036 to 2065 and the late century from 2069 to 2098. Both future scenarios as well as the baseline period were forced by the bias corrected GCM-RCM outputs. This procedure was applied for both the runs calibrated using MDC and Q_{only} calibration.

4. Results

4.1. Multi-dataset calibration

4.1.1. Bias-correction of climate model data

The changes induced by applying quantile mapping to climate model simulations are shown for the HadCM3Q0-ETHZ_CLM combination as an example (Fig. 2). The GCM-RCM simulations during the baseline period (RCM 1980–2009 raw) with a 25 km resolution were corrected using reference observations from the same period (OBS 1980–2009), resulting in the same annual cycle (RCM 1980–2009 cor.). The same correction was then applied to future simulations resulting in the quantile mapped climate scenario from 1951 to 2099. In this example the late century period as an excerpt of the entire result is shown (RCM 2070–2009 cor.). The mean difference of each day of the observations and the scenario as well as the ratio of the standard deviations of the scenarios and the simulations indicate the goodness of fit after the bias correction (Table 2).

The different bias-corrected GCM-RCM projections of temperature and precipitation reveal significant differences (Fig. 3). All models agree on rising temperatures but they differ in the extent of the increase. The projected temperature increase is larger during the melt season than during winter. This difference becomes more significant in the late century. On average, precipitation is projected to slightly decrease during the melt season. During the low flow season, especially in the far term, the spread in precipitation is largely increased by the simulations driven by ECHAM, which is in line with findings from the nearby Vispa valley (Finger et al., 2012).

4.1.2. MDC – parameter ensemble selection

The scores of the different ensembles of parameter sets were evaluated by comparing their scores in all five objective functions. The performance of the ten best parameter sets using all possible combinations of the datasets was then evaluated using the P^{OAnorm} efficiency criteria (Fig. 4). A first finding of the multi-dataset calibration is that the score of the overall consistency performance increases if more datasets are added to the calibration procedure. Consequently, the highest score is reached when the model calibration was performed using the combination of all three datasets. However, the efficiency criteria in section 3.1.3 for the single datasets were not necessarily highest when all datasets were combined. However, the consistency of a simulation is higher when at least two datasets are combined in almost all cases and highest when all three datasets are combined, even though the single objective functions do not reach their overall maximum. An exception is the calibration to Q and SC, which yields lower P^{OAnorm} than the calibration to Q_{only} due to a poor representation of MB values. Given that Q and MB were derived from respectively lake level observations and large scale modelling, their value regarding the improvement of P^{OAnorm} has to be considered with precaution.

Therefore, we chose the ten parameter sets calibrated to Q, SC and MB for the model calibration (see Fig. 4), as well as the ten parameter sets obtained by calibration to Q_{only} for comparison.

4.1.3. Model validation

The results of the model runs with the ten best parameter sets (see Section 4.1.2) are satisfying (Fig. 5). The discharge is represented adequately during the calibration and validation periods. However, there are some peaks in the simulation, which do not exist in the observed data, or at least not as prominently. These occur mainly during winter (e.g. early 2001, 2002, 2004, 2005, 2006, 2008 and late 2007). Generally, the model rather underestimates the runoff during the melt season and overestimates the runoff in

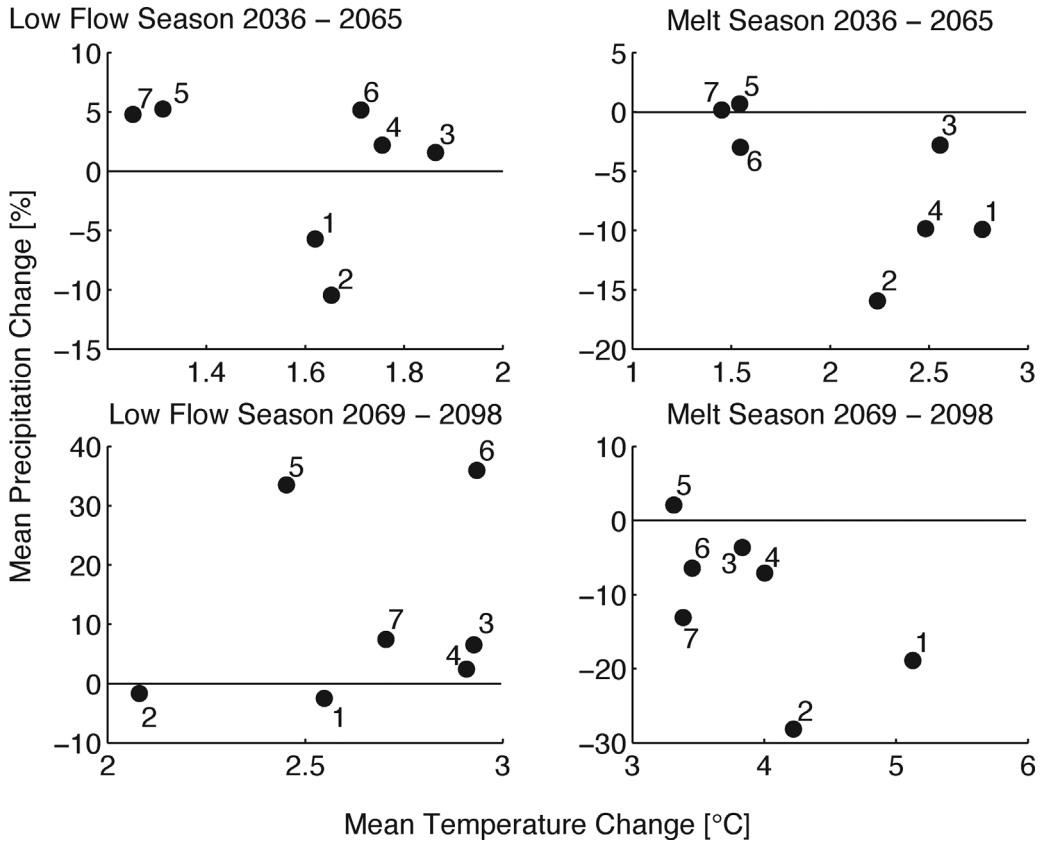


Fig. 3. Climate change signals in mean air temperature and precipitation, for the middle of the century (2036–2065) and the late century (2069–2098) compared to the reference period (1980–2009) scenario during low flow (January to April) and melt season (May to September). Labels indicate specific climate scenarios as listed in Table 2.

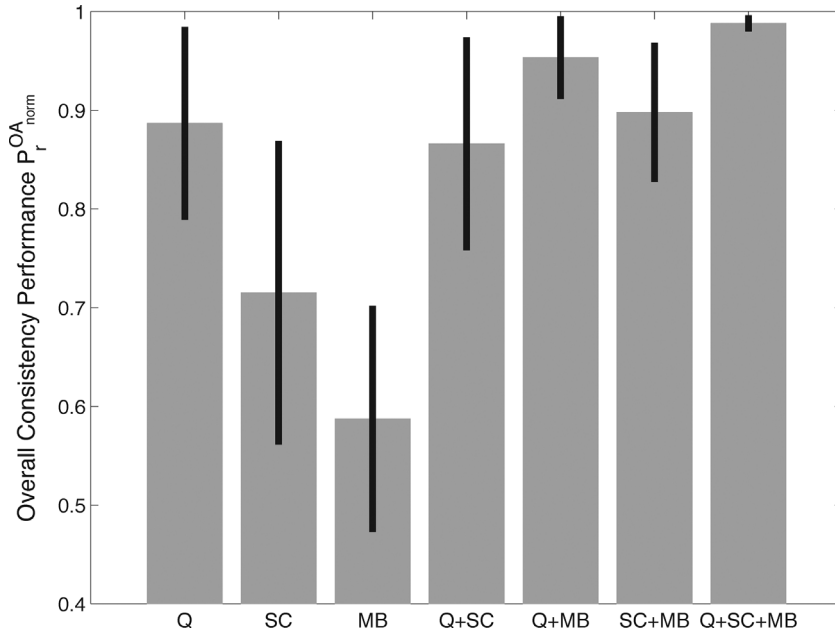


Fig. 4. Multi-dataset calibration results represented by the overall consistency performance $P_r^{OA_{norm}}$. The different parameter set ensembles are compared when calibrating to different combinations of objective functions. Q stands for calibration to discharge (using NSE and LogNSE), SC for calibration to snow cover (using CPSCy and CPSCs) and MB stands for calibration to glacier mass balances (using MBRmse). Vertical bars represent the standard deviation.

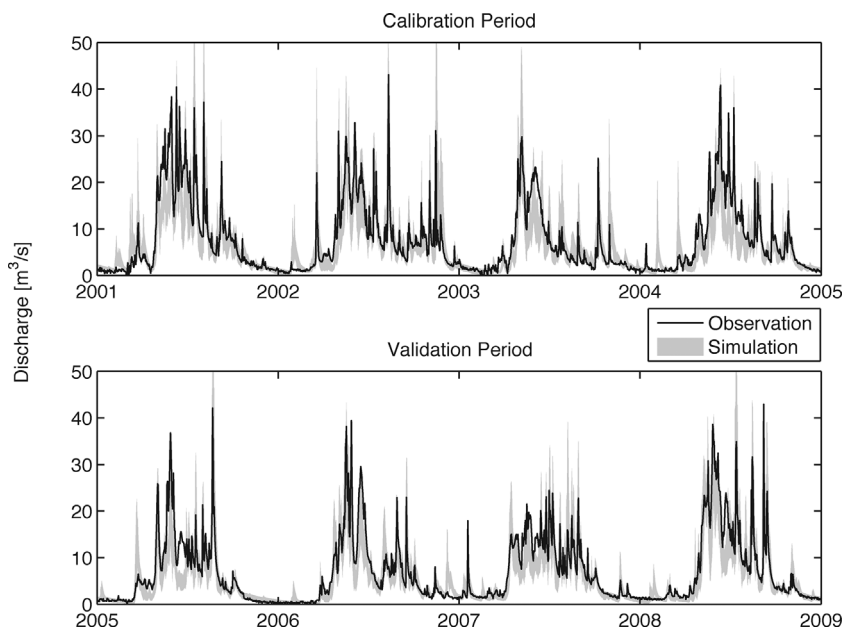


Fig. 5. Observed (black) and modelled discharge (grey) during the calibration (2001–2004) and the validation period (2005–2008) using the ten best parameter sets of the MDC calibration.

fall and early winter. The biggest absolute model errors during both the calibration and the validation period occur during the May and June when all runoff processes occur at the same time.

As can be seen from the objective function scores in Table 3, the discharge simulation performance was slightly decreased using the MDC at the expense of the snow cover and the glacier mass balance representation. This was to be expected and confirms the results of the calibration in Fig. 4.

The accuracy in the average snowcover simulations with the MDC and the Q_{only} ensemble parameter sets (Fig. 6) is variable throughout the year. It is worst in October. The mean of the simulated area, however, matches the observations relatively well. Most inaccuracies occur during the periods of snow melt and the first snowfall in autumn. Fig. 6 reveals that the snow-covered area, especially during the summer months, is often overestimated by about 10 % in the Q_{only} calibration. The same tendency is also visible for the MDC, however it is not as extreme. This can be verified by comparing the objective function scores of the snow cover representation in Table 3, where the improvement in the summer metric (CPSCs) is bigger than in the annual one (CPSCy).

4.2. ANOVA

The ANOVA-based uncertainty analysis reveals that the variance is mainly driven by the seven climate scenarios in Table 2. The contribution of the climate scenario ensemble to the total uncertainty dominates the discharge simulation Fig. 7. The ten parameter sets contribute most to the overall uncertainty during the summer months (around 15–20%). The contribution of the glacier scenarios is vanishingly small in the middle of the century and is not visible in Fig. 7. In the late century-scenario glaciers were therefore not incorporated. The variance fraction attributed to the interactions and errors is biggest in winter (around 20%). Between the two there is no significant difference, even though there are no glaciers in the late century period. However, the influence of the parameter sets becomes slightly smaller in the late century period during the whole year apart from June and July.

Table 3
Objective function scores in of the model validation for the multi dataset calibration (MDC) and the calibration to discharge only (Q_{only}).

	Q_{only}	MDC
NSE	0.76	0.69
LogNSE	0.78	0.74
CPSCy	0.87	0.88
CPSCs	0.86	0.88
MB _{RMSD}	0.02	0.04

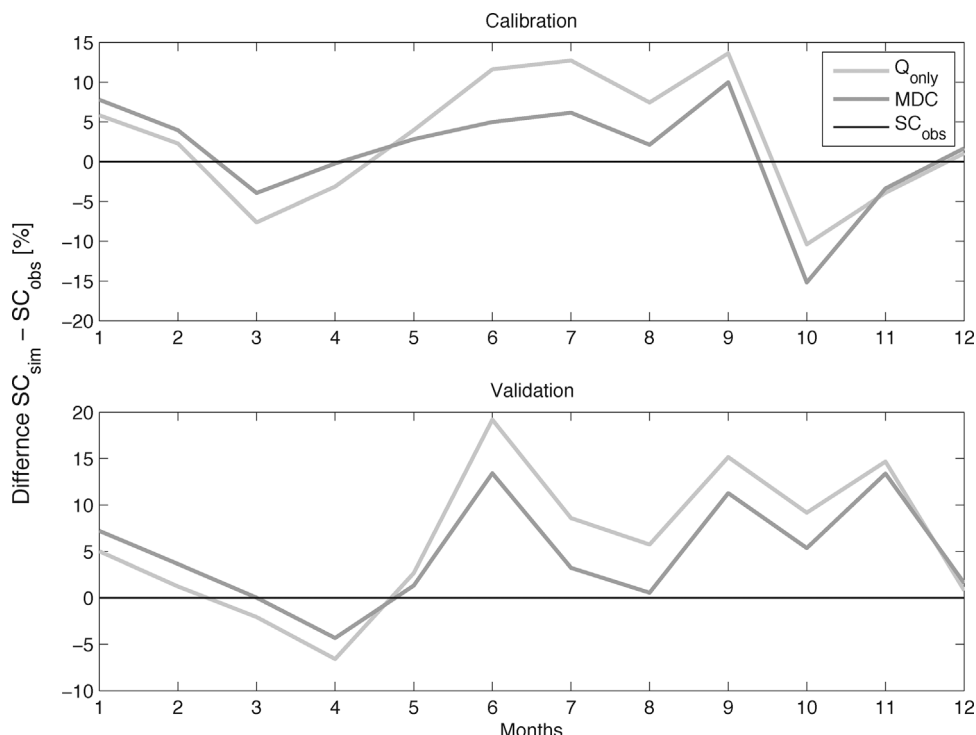


Fig. 6. The differences in snowcover simulation between the observations (SC_{obs}) and the simulations during the calibration and validation period with the ten MDC and the ten Q_{only} parameter sets. Values are given in percentage of snow covered area of the catchment.

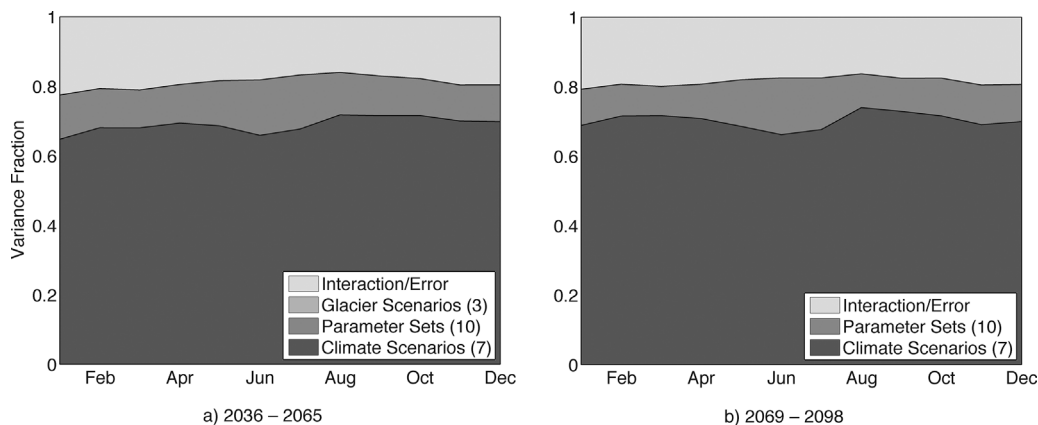


Fig. 7. Result of the analysis of variance (ANOVA) for (a) the middle of the century and (b) the late century period. Note that the uncertainty attributed to the three glacier scenarios is too small to appear in (a). The numbers in brackets represent the number of data or parameter sets used for model calibration.

4.3. Discharge scenarios

4.3.1. Future runoff

Fig. 8 shows the mean modelled discharge with its standard deviation from the three main sources: (i) rain, (ii) snow melt and (iii) glacier melt water during the baseline period and over 30 years of simulation in the middle and late century periods. The results are shown for the scenarios using both the MDC and the Q_{only} calibration.

The results of both calibrations procedures (Fig. 8) indicate that the total discharge becomes more and more evenly distributed in the future periods. Furthermore, the stretched peak of discharge in May and June in the baseline period will probably become less prominent in the middle of the century and will have disappeared into a single peak in May by the end of the century. According to the simulations, there will be an increase in discharge in winter due to an increasing contribution of rain water and snow melt water. During the summer months the overall discharge tends to be smaller since runoff from both rain and snow melt is declining. Rain water is projected to increase the total runoff again during late fall and winter. The contribution from melting glacier ice is biggest in the months July to September, it declines however rapidly in the middle of the century as these small glaciers are expected to have

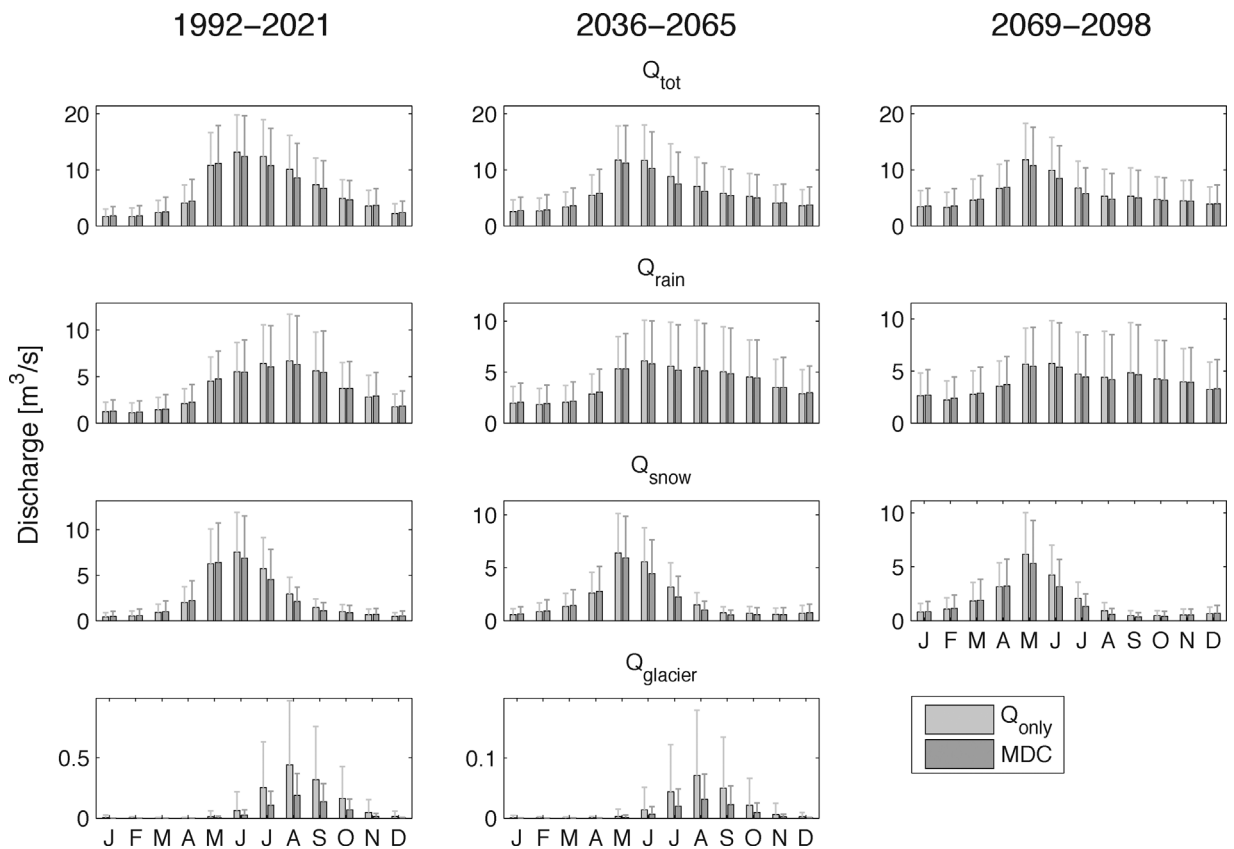


Fig. 8. The total runoff (Q_{tot}) in the baseline (1992–2021), the middle of the century (2035–2064) and end of century (2069–2098) periods for the calibration to runoff only (Q_{only} – in light grey) and the calibration to multiple datasets (MDC – in dark grey). The runoff is furthermore split up into the different sources of runoff: rain (Q_{rain}), snow melt (Q_{snow}), and glacial melt water ($Q_{glacier}$). Whiskers indicate the standard deviation of the ensemble based on the combination of 10 parameter sets, 7 climate scenarios and 3 glacier scenarios.

disappeared by the mid-21st century (Huss and Fischer, 2016; Fig. 8).

4.3.2. Q_{only} vs MDC

The results of the two different calibration procedures indicate the most striking difference is in the discharge quantities from glacial melt. In the baseline and the middle of the century period, the MDC helps to reduce the mean annual uncertainty in the glacier runoff projections by 97 and 65 %, respectively (bottom row of Fig. 8). Furthermore, the mean annual modelled glacial melt discharge using the Q_{only} calibration is almost double the predicted runoff using the MDC calibration in both periods, and thus likely to be unrealistic. The same holds true for the middle of the century period, although the projected glacial melt-runoff is already projected to be below $0.1 \text{ m}^3 \text{ s}^{-1}$ and thus has to be interpreted with caution.

In the projections of the contributions of rain and snow melt water, the standard deviations of both calibration techniques are about the same size. However, the amounts of runoff are constantly different for the two techniques. In periods of high snow melt and rain runoff amounts, the Q_{only} calibration produces consistently higher runoff volumes than the MDC. In periods with lower discharge the opposite happens. This pattern is propagated into the total discharge.

4.3.3. Future snow cover extent

The snowcover simulations of the MDC simulations indicate that the catchment will be entirely snow-free over longer periods in the future based on monthly averages. The projections in Fig. 9 show a decline in snow-covered area during the winter and longer periods with less or even no snow compared to today.

Fig. 10 demonstrates the relative changes of the total discharge in the two future periods using the MDC calibration. As already depicted in Fig. 8, the discharge increases from November to April and decreases from June to September. The projected changes are bigger than the associated standard deviations in the months of January to April, July, August and December in the middle of the century and additionally also in June in the late century. In the remaining months the direction of the change is not entirely certain. However, the trends for both periods are the same, but in the late century period, they become more significant. Table 4 shows the changes in total annual discharge specified according to its different sources in the middle and the late century periods. Overall discharge shows a slightly decreasing trend in the mean over all ensemble runs, however the standard deviation exceeds this change

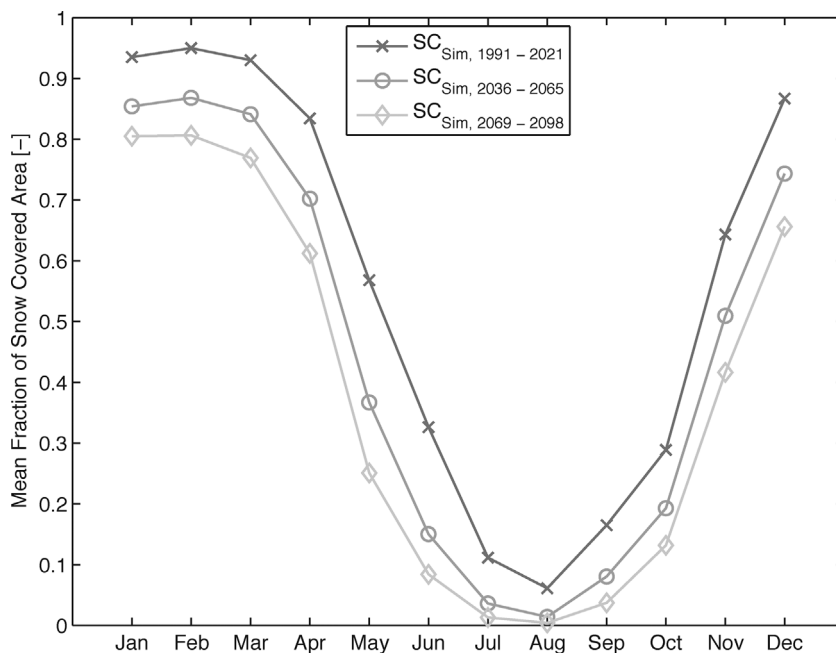


Fig. 9. Comparison of the mean monthly snow covered area predictions in the baseline, middle and late century scenarios.

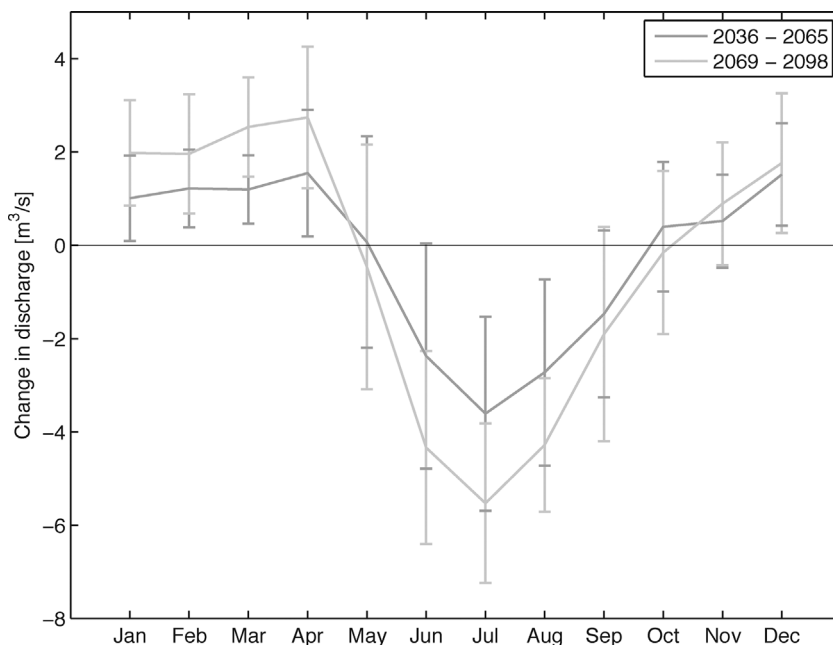


Fig. 10. The modelled change in discharge in the middle and the late century scenarios compared to the baseline scenario 1992–2021. The vertical bars indicate the standard deviation of the change signal.

by almost a factor of four in the middle and a factor of three in the late century scenario. This indicates that the finding of decreasing annual runoff in the future is not robust. The discharge derived from rain is projected to increase by 8–10% but the uncertainties are considerable. For the snowcover the trend is in the opposite direction. The decreases in melt water from snow melt are projected to be between 20 and 29 %, respectively. These changes are significant but their magnitude is highly uncertain. The most significant change occurs for runoff due to glacier ice melt water with a mean decrease of 83 % in the middle of the century period relative to the baseline period.

Table 4

Future annual discharge sums in the middle and the late century in millions of m³ per year and the mean changes in percent and their standard deviation compared to the baseline period.

Runoff component	1992–2021			2036–2065		2069–2098	
	Mm ³ yr ⁻¹	Mm ³ yr ⁻¹	%	Mm ³ yr ⁻¹	%	Mm ³ yr ⁻¹	%
Q _{sim} total	208	201	-4 ± 15	195	-6 ± 18		
Q _{sim} , rain	126	136	+8 ± 23	138	+10 ± 26		
Q _{sim} , snow	80	64	-20 ± 19	57	-29 ± 21		
Q _{sim} , glacier	2	0.3	-83 ± 18	0	0		

5. Discussion

5.1. Multi-dataset calibration

We applied an innovative calibration approach relying on multiple datasets. However, these datasets all are subject to uncertainties. The discharge into Gigerwaldsee was not measured directly but was derived from the observed water balance in the reservoir and thus exhibits an uncertainty that is difficult to quantify. Given that MODIS-based snow cover maps in the Alps are subject to an estimated uncertainty of around 10% (Finger et al., 2015) and glacier mass balances also have uncertainties of around 10% (Huss et al., 2010), we decided to attribute the same weight to all three observational datasets. These datasets were then used to find the ten best parameter sets of the calibration of the HBV-light model. The selection of exactly ten parameter sets does not consider the differences in performance from one parameter set to another, but on the other hand, results in a fixed number of parameter sets. The calibration to multiple datasets indicated an increase in the overall model consistency in our case as well as in the literature (Finger et al., 2015, 2011; Juston et al., 2009). There was, however, one exception: The calibration to Q and SC resulted in a comparably poor representation of the annual glacier mass balances. While Q and MB were derived from lake level observations and large scale modelling, respectively, SC was directly obtained from MODIS imagery (Hall et al., 2002). Accordingly, performance regarding Q and MB may also be attributed to uncertainty in the reference dataset used for calibration. Furthermore, tests showed that if the 100 best parameter sets would have been selected, the Q and SC simulations would also perform better than the calibration to discharge only. Nevertheless, we decided to stick to a selection of the ten best parameter sets, since this results in a higher overall performance in all combinations. In the end, the MDC leads to a better simulation of the snow-covered extent compared to the Q_{only} calibration (see Fig. 6) and therefore also to an improved model consistency, yet at the expense of slightly lower performance of the discharge simulation. Unlike projections in heavily glacierized catchments, like e.g. in the Himalayas (Immerzeel et al., 2012), glacier retreat scenarios have little impact on projections of future total runoff in catchments with very small glacierization. In consequence, the behaviour of the snow cover is more crucial in terms of runoff production. Furthermore, MDC revealed to reduce simulated snow accumulation in high altitude areas to an acceptable level for decadal simulation, making the model results more realistic and hence suitable for climate change projections (Finger et al., 2015).

The overall representation of discharge is satisfying. The errors during the period of highest flow can be explained by the fact that the total runoff at this time is maximal with considerable fluctuations and also because all runoff processes such as rain, glacier melt and snow melt occur at the same time. Furthermore, the discharge over the periods used for calibration and validation can be substantially different in these months. Reinforcing effects in the model can also explain errors in discharge representation: for example, too high temperatures result in a snowcover that is too small and therefore the model produces too little streamflow or at the wrong point in time. This can be seen in Fig. 6, where the minimal snow coverage in summer in the model is often reached later compared to the observations. Discharge from snow melt in spring is thus too low as the model underestimates snow melt. The missed peaks during the calibration and validation period in Fig. 5 could be attributed to such an erroneous snowmelt representation. This can however not be tested, since no separation of the origin of the water flowing into the lake has been performed. To simulate snow cover more realistically, it might have been beneficial to include data on the snow water equivalent into HBV. However, this quantity strongly varies. Even local measurements have uncertainties of between 13 and 30% (Jonas et al., 2009). Since no consistent long-term dataset on snow water equivalent is available for the Gigerwald valley, we use time series of the on snow covered area for model calibration. In the end, the poor model performance in spring might have its roots in a combination of different issues in the model such as an inaccurate temperature threshold for melt triggering or overestimated evapotranspiration due to the temperature based method. Finally, flaws in the measurements and interpolation techniques of the weather datasets can introduce errors, which might then be propagated into the model calibration or via the bias correction into the climate scenarios.

5.2. ANOVA

The results of the ANOVA show that the glacier scenarios do not contribute to the total uncertainty within the model results. Unlike in catchments with higher degrees of glacierization (Finger et al., 2012) the climate scenarios introduce the highest uncertainties throughout the entire year, which is consistent with the findings of Addor et al. (2014), Bosshard et al. (2013), and Vetter et al. (2017). Furthermore, although this is not explicitly accounted for in this study, the choice of the emission scenario is an important source of uncertainty by the end of the century, particularly in alpine catchments (Addor et al., 2014). Even within a

particular emission scenario it is still uncertain how the redistribution of rainfall in the different seasons will change (Swiss Federal Office for the Environment, 2012). Looking at Fig. 3, these uncertainties can also be identified in the emission scenario that was used in the present study. Propagating these uncertainties through hydrological models nevertheless provides valuable insights into future changes in the water balance under climate change. Finally, the multi-dataset calibration approach should also be tested using other datasets like snow heights, evapotranspiration and ground water levels. The uncertainties involved in the modelling process are difficult to quantify and special focus should also be laid upon uncertainties in the observational datasets and how they are propagated through the model.

5.3. Discharge scenarios

5.3.1. Benefits of applying an MDC

In order to produce realistic projections of runoff in alpine areas under future climate scenarios, it is essential that the model can realistically capture the main runoff sources, i.e. snow cover observations, glacier mass balances and direct runoff. The overall consistency performance quantifies the simultaneous simulation of these datasets (Finger et al., 2012). In this paper we extended the application of a MDC to future scenarios using a conceptual model. We showed that the model consistency is improved compared to the more traditional Q_{only} calibration (Fig. 8). This is especially relevant for the representation of snow cover, for which the benefit of using MDC became visible during the calibration and validation periods of the model (Fig. 6). The glaciers in this catchment are very small. Nevertheless, we decided to still use the glacier mass balances for calibration, since they have considerable skill in informing about temporal changes in ice and snow water equivalent and thus melt water volumes and, hence, support the model in more realistically simulating all processes. Furthermore, glacier mass balance data allowed demonstrating the benefit of MDC, such as its influence on the projections for the different runoff sources: The increase in overall discharge in the Q_{only} calibration compared to the MDC is mainly induced by the increased snow melt of about 10 % in the Q_{only} compared to the MDC calibration.

The glaciers in this catchment are too small to produce runoff which significantly influences the total runoff. However, the uncertainties within the glacial runoff projections could be drastically reduced using the MDC projections. The glacial melt runoff even decreased by 95 % in the MDC compared to the Q_{only} calibration (Fig. 8). This effect is most striking when the glaciers still cover a relevant area, i.e. during the baseline period. Even though the glacial melt runoff is comparably small, its representation in the simulation is valuable to show the benefits of the MDC. A substantial overestimation of snow melt might result in simulations with too much total runoff in the future when using a Q_{only} calibration. Such erroneous predictions could lead to substantial misinvestments and in non-adequate infrastructure adaptations for climate change mitigation by the hydropower companies.

5.3.2. Impacts on hydrology

To assess the impacts of climate change calculated using the MDC compared to the present state of the catchment, we analysed the changes between the baseline period (1992–2021) representing present state and the two future periods (2036–2065 and 2069–2098) and identified the trends. The projected changes of runoff in winter and summer are larger than their standard deviations (Fig. 10). The standard deviations that exceed the mean projected change rates during late spring and fall can, besides the large uncertainties in the climate projections as revealed in the ANOVA, to a certain extent be attributed to the small degree of glacierization in the catchment, because a smaller degree of glacierization leads to less distinct changes in the future (Farinotti et al., 2012).

The projections of the total annual discharge indicate a decreasing trend, which is however not significant (Table 4). Similar trends were found by van Vliet et al. (2016) on a global scale, and had previously already been confirmed by several studies in the European Alps (e.g. Farinotti et al. (2012) and Gaudard et al. (2013)). We assume that the decrease in overall annual runoff is driven by an increase in evaporation along with slightly smaller amounts of total precipitation projected by the scenarios. Studies on much larger scales in China and an Amazon tributary showed that even increases in precipitation in combination with increasing temperatures can lead to decreased stream flow (Fu et al., 2009; Mohor et al., 2015). Kopytkovskiy et al. (2015) mention increased air temperatures and therefore also increasing evaporation as the main reason for decreasing runoff, which is projected to occur mainly during the summer months in the Colorado River basin in the US under the emission scenarios A2 and B1. Increasing runoff up to the middle of the century are projected for glacierized basins of the Himalaya and Karakoram mountain ranges due to more precipitation and intensified glacier melt (Lutz et al., 2014).

The Calfeisental and its tributary from the Weisstannental include only a few very small glaciers and accordingly the retreating of glaciers due to a warming climate will not have a significant impact on future discharge projections. Nevertheless, the peak discharge is projected to occur earlier in spring, since it will increasingly depend on snowmelt and rain.

Furthermore, our study shows increasing discharge during the winter months due to higher temperatures and increasing precipitation falling as rain. Due to higher temperatures, the snow melts faster in spring which further enhances the effect of earlier occurring peak discharges in spring with higher peak flows. This shift has been also been predicted by Nohara et al. (2006) for several streams at high latitudes in the Northern Hemisphere, Bavay et al. (2009, 2013) for snow dominated catchments in the eastern Swiss Alps, and by Kopytkovskiy et al. (2015) in the Colorado River basin in summer, after the ablation season, discharge is projected to strongly decrease. Besides a lack in snow-covered area and glaciers that could provide runoff, less rainfall enhances this effect. Together with higher temperatures we can also expect more evapotranspiration and therefore less water is routed into the runoff. Towards fall, the rainfall increases again and thus also runoff compared to the present state as well as the overall runoff attributed to rain.

Our results indicate that the hydropower company in the Calfeisental might have to adapt their management scheme to increased runoff in fall and winter and to deal with a drastically reduced amount of water due to less snow available for melt in summer. The

MDC yields more realistic and reliable simulations of the contribution of rain, snow melt and glacial melt to total runoff. For the hydropower company, our results for example allow better classifying the consequences of the likely disappearance of glaciers in the near future. Our study shows that a loss of all the glaciers in the catchment does not necessarily lead to significant impacts on the available water quantities, nor the seasonal distributions. Furthermore in extreme years with a limited snow cover in the catchment, our results provide clear indications for the hydropower company how much runoff is to be expected from rain. Although these quantities can also be obtained from hydrological models calibrated to discharge only, we argue that those results are questionable if the other contributors to the total runoff are neglected during model calibration and might yield results being subject to a potential error compensation. Moreover the applied method allows us to put more trust in the simulation of rather negligible contributors to the total runoff. This in turn allows a much more detailed prediction of the future runoff composition.

To our knowledge no study has been published so far that combines a multi-dataset calibration and climate scenarios in a semi-distributed hydrological model. We explored this approach for conceptual models. Since these models have a smaller need for input data and are computationally less demanding, multiple model runs using large ensembles of parameter sets can be performed efficiently. Together with recent advances in remote sensing techniques to obtain glacier mass balances (Dehecq et al., 2016) and snow cover information (Gafurov et al., 2016; Hall et al., 2002) including the knowledge about how many discharge measurements are needed in order to calibrate a hydrological model (Seibert and Beven, 2009), this approach facilitates the realisation of similar studies also in more remote regions.

6. Conclusions

In this study, we combined a multi-dataset calibration with a quantile mapped ensemble of climate scenarios in order to produce discharge scenarios for the watershed of Gigerwaldsee. We showed that a hydrological model calibration to multiple datasets, which can be obtained by using freely available remote sensing imagery, improves the realism of results, such as e.g. the representation of the snow covered area. By calibrating the model to multiple reference datasets, the internal model structure is forced to represent the catchment processes more accurately, which contributes to more reliable simulations under future climate. real-world consistency of the simulation results

A simulation using ten equifinal parameter sets, seven climate model outputs and three glacier scenarios produced an ensemble of 210 discharge scenarios until the middle of the 21st century. For the second half of the century, glaciers were not taken into account since our simulations indicate that they will have disappeared. Most of the uncertainty in the projections was introduced by the differences between the climate scenarios, whereas the contribution of the different parameter sets is comparatively small. The contribution of glacial melt to the resulting uncertainty and to total runoff proved to be negligible. However, the uncertainty in the glacial runoff was greatly reduced by applying the multi-dataset calibration. This in turn allows us to put more trust into the predictions of the single contributors to the total runoff.

The future annual runoff into the Gigerwaldsee will be more evenly distributed throughout the year compared to an average year of the baseline period. Winter discharge is projected to increase significantly and in summer, from June to September, there will be significantly less runoff. In spring the occurrence of the peak discharge will occur earlier in the year due to earlier snow melt. Furthermore, the amount of snowmelt water will decline in the middle and the late century, because more precipitation will fall as rain and rapidly contribute to runoff. This means that in a catchment with a very low degree of glacierization, the correct representation of the snowcover is decisive for reliable runoff projections. We hence focussed on the accurate representation of snow accumulation and melting processes, since their timing is crucial for the management of hydropower facilities. Overall we see multi-dataset calibration approaches such as the one employed in this study as promising tools to improve the realism of hydrological processes in impact assessments and to support decision making on investments into new hydropower structures.

Acknowledgements

J. Seibert and M. Vis provided important support regarding the application of the HBV-light model. We furthermore want to thank Kirsti Hakala for providing valuable comments on the selection of climate models. We also acknowledge the Kraftwerke Sarganserland AG for the discharge data, MeteoSwiss for the gridded weather datasets and the EU-funded FP6 Integrated Project ENSEMBLES for the climate projections. Comments by two anonymous reviewers helped to improve the manuscript.

References

- Addor, N., Fischer, E.M., 2015. The influence of natural variability and interpolation errors on bias characterization in RCM simulations. *J. Geophys. Res. Atmos.* 120 (180–10), 195. <http://dx.doi.org/10.1002/2014JD022824>.
- Addor, N., Seibert, J., 2014. Bias correction for hydrological impact studies – beyond the daily perspective. *Hydrol. Process.* 28, 4823–4828. <http://dx.doi.org/10.1002/hyp.10238>.
- Addor, N., Rössler, O., Köplin, N., Huss, M., Weingartner, R., Seibert, J., 2014. Robust changes and sources of uncertainty in the projected hydrological regimes of Swiss catchments. *Water Resour. Res.* 50, 7541–7562. <http://dx.doi.org/10.1002/2014WR015549>.
- Barnett, T.P., Adam, J.C., Lettenmaier, D.P., 2005. Potential impacts of a warming climate on water availability in snow-dominated regions. *Nature* 438, 303–309. <http://dx.doi.org/10.1038/nature04141>.
- Bauder, A., Funk, M., Huss, M., 2007. Ice-volume changes of selected glaciers in the Swiss Alps since the end of the 19th century. *Ann. Glaciol.* 46, 145–149. <http://dx.doi.org/10.3189/172756407782871701>.
- Bavay, M., Lehning, M., Jonas, T., Löwe, H., 2009. Simulations of future snow cover and discharge in Alpine headwater catchments. *Hydrol. Process.* 23, 95–108. <http://dx.doi.org/10.1002/hyp.7195>.

- Bavay, M., Grünewald, T., Lehning, M., 2013. Response of snow cover and runoff to climate change in high Alpine catchments of Eastern Switzerland. *Adv. Water Resour.* 55, 4–16. <http://dx.doi.org/10.1016/j.advwatres.2012.12.009>.
- Beldring, S., Engeland, K., Roald, L.A., Sælthun, N.R., Voksø, A., 2003. Estimation of parameters in a distributed precipitation-runoff model for Norway. *Hydrol. Earth Syst. Sci.* 7, 304–316. <http://dx.doi.org/10.5194/hess-7-304-2003>.
- Beniston, M., Stoffel, M., Hill Clarvis, M., Quevauviller, P., 2014. Assessing climate change impacts on the quantity of water in Alpine regions: foreword to the adaptation and policy implications of the EU/FP7 ACQWA project. *Environ. Sci. Policy* 43, 1–4. <http://dx.doi.org/10.1016/j.envsci.2014.01.009>.
- Beven, K., Binley, A., 1992. The future of distributed models: model calibration and uncertainty prediction. *Hydrol. Process.* 6, 279–298. <http://dx.doi.org/10.1002/hyp.3360060305>.
- Bosshard, T., Carambia, M., Goergen, K., Kotlarski, S., Krahe, P., Zappa, M., Schär, C., 2013. Quantifying uncertainty sources in an ensemble of hydrological climate-impact projections. *Water Resour. Res.* 49, 1523–1536. <http://dx.doi.org/10.1029/2011WR011533>.
- Boughton, W.C.A., 1966. A mathematical model for relating runoff to rainfall with daily data. *Civ. Eng. Trans. Inst. Eng. Aust.* CE81, 83–97.
- CH2014, 2014. *Toward Quantitative Scenarios of Climate Change Impacts in Switzerland*, Published by OCCR, FOEN, MeteoSwiss, C2SM, Agroscope and ProClim, Bern, Switzerland.
- Christensen, J.H., Boberg, F., Christensen, O.B., Lucas-Picher, P., 2008. On the need for bias correction of regional climate change projections of temperature and precipitation. *Geophys. Res. Lett.* 35, L20709. <http://dx.doi.org/10.1029/2008GL035694>.
- Dehecq, A., Millan, R., Berthier, E., Gourmelen, N., Trounev, E., Vionnet, V., 2016. Elevation changes inferred from TanDEM-X data over the Mont-Blanc area: impact of the X-band interferometric bias. *IEEE J. Sel. Top. Appl. Earth Obs. Remote Sens.* 9, 3870–3882. <http://dx.doi.org/10.1109/JSTARS.2016.2581482>.
- Farinotti, D., Usselmann, S., Huss, M., Bauder, A., Funk, M., 2012. Runoff evolution in the Swiss Alps: projections for selected high-alpine catchments based on ENSEMBLES scenarios. *Hydrol. Process.* 26, 1909–1924. <http://dx.doi.org/10.1002/hyp.8276>.
- Field, C.B., Barros, V.R., Mach, K.J., Mastrandrea, M.D., van Aalst, M., Adger, W.N., Arent, D.J., Barnett, J., Betts, R., Bilir, T.E., Birkmann, J., Carmin, J., Chadee, D.D., Challinor, A.J., Chatterjee, M., Cramer, W., Davidson, D.J., Estrada, Y.O., Gattuso, J.-P., Hijikata, Y., Hoegh-Guldberg, O., Huang, H.Q., Insarov, G.E., Jones, R.N., Kovats, R.S., Romero-Lankao, P., Larsen, J.N., Losada, I.J., Marengo, J.A., McLean, R.F., Mearns, L.O., Mechler, R., Morton, J.F., Niang, I., Oki, T., Olwoch, J.M., Opondo, M., Poloczanska, E.S., Pörtner, H.-O., Redster, M.H., Reisinger, A., Revi, A., Schmidt, D.N., Shaw, M.R., Solecki, W., Stone, D.A., Stone, J.M.R., Strzepek, K.M., Suarez, A.G., Tschakert, P., Valentini, R., Vicuña, S., Villamizar, A., Vincent, K.E., Warren, R., White, L.L., Wilbanks, T.J., Wong, P.P., Yohe, G.W., 2014. Technical summary. *Climate Change 2014: Impacts, Adaptation, and Vulnerability. Part A: Global and Sectoral Aspects. Contribution of Working Group II to the Fifth Assessment Report of the Intergovernmental Panel on Climate Change*. Field, C.B., V.R. Ba, Cambridge University Press Cambridge, United Kingdom and New York, NY, USA.
- Finger, D., Pellicciotti, F., Konz, M., Rimkus, S., Burlando, P., 2011. The value of glacier mass balance, satellite snow cover images, and hourly discharge for improving the performance of a physically based distributed hydrological model. *Water Resour. Res.* 47. <http://dx.doi.org/10.1029/2010WR009824>.
- Finger, D., Heinrich, G., Gobiet, A., Bauder, A., 2012. Projections of future water resources and their uncertainty in a glacierized catchment in the Swiss Alps and the subsequent effects on hydropower production during the 21st century. *Water Resour. Res.* 48. <http://dx.doi.org/10.1029/2011WR010733>.
- Finger, D., Vis, M., Huss, M., Seibert, J., 2015. The value of multiple data set calibration versus model complexity for improving the performance of hydrological models in mountain catchments. *Water Resour. Res.* 51, 1939–1958. <http://dx.doi.org/10.1002/2014WR015712>.
- Fischer, M., Huss, M., Barboux, C., Hoelzle, M., 2014. The new Swiss glacier inventory SGI2010: relevance of using high-resolution source data in areas dominated by very small glaciers. *Arctic, Antarct. Alp. Res.* 46, 933–945. <http://dx.doi.org/10.1657/1938-4246-46.4.933>.
- Fischer, M., Huss, M., Hoelzle, M., 2015. Surface elevation and mass changes of all Swiss glaciers 1980–2010. *Cryosph* 9, 525–540. <http://dx.doi.org/10.5194/tc-9-525-2015>.
- Franks, S.W., Gineste, P., Beven, K.J., Merot, P., 1998. On constraining the predictions of a distributed model: the incorporation of fuzzy estimates of saturated areas into the calibration process. *Water Resour. Res.* 34, 787–797. <http://dx.doi.org/10.1029/97WR03041>.
- Frans, C., Istanbuloglu, E., Lettenmaier, D.P., Naz, B.S., Clarke, G.K.C., Condom, T., Burns, P., Nolin, A.W., 2015. Predicting glacio-hydrologic change in the headwaters of the Zongo River, Cordillera Real, Bolivia. *Water Resour. Res.* 51, 9029–9052. <http://dx.doi.org/10.1002/2014WR016728>.
- Frei, C., Schär, C., 1998. A precipitation climatology of the Alps from high-resolution rain-gauge observations. *Int. J. Climatol.* 900, 873–900.
- Frei, C., Schöll, R., Fukutome, S., Schmidli, J., Vidale, P.L., 2006. Future change of precipitation extremes in Europe: intercomparison of scenarios from regional climate models. *J. Geophys. Res.* 111. <http://dx.doi.org/10.1029/2005JD005965>.
- Frei, C., 2014. Interpolation of temperature in a mountainous region using nonlinear profiles and non-Euclidean distances. *Int. J. Climatol.* 34, 1585–1605. <http://dx.doi.org/10.1002/joc.3786>.
- Fu, G., Charles, S.P., Yu, J., Liu, C., 2009. Decadal climatic variability, trends, and future scenarios for the North China plain. *J. Clim.* 22, 2111–2123. <http://dx.doi.org/10.1175/2008JCLI2605.1>.
- Gafurov, A., Lüdtkke, S., Unger-Shayesteh, K., Vorogushyn, S., Schöne, T., Schmidt, S., Kalashnikova, O., Merz, B., 2016. MODSNOW-tool: an operational tool for daily snow cover monitoring using MODIS data. *Environ. Earth Sci.* 75, 1078. <http://dx.doi.org/10.1007/s12665-016-5869-x>.
- Gaudard, L., Gilli, M., Romero, F., 2013. Climate change impacts on hydropower management. *Water Resour. Manag* 27, 5143–5156. <http://dx.doi.org/10.1007/s11269-013-0458-1>.
- Gaudard, L., Romero, F., Dalla Valle, F., Gorret, R., Maran, S., Ravazzani, G., Stoffel, M., Volonterio, M., 2014. Climate change impacts on hydropower in the Swiss and Italian Alps. *Sci. Total Environ.* 493, 1211–1221. <http://dx.doi.org/10.1016/j.scitotenv.2013.10.012>.
- Geris, J., Tezlauff, D., Seibert, J., Vis, M., Soulsby, C., 2015. Conceptual modelling to assess hydrological impacts and evaluate environmental flow scenarios in montane river systems regulated for hydropower. *River Res. Appl.* 31, 1066–1081. <http://dx.doi.org/10.1002/rra.2813>.
- Gudmundsson, L., Bremnes, J.B., Haugen, J.E., Engen-Skaugen, T., 2012. Technical note: downscaling RCM precipitation to the station scale using statistical transformations – a comparison of methods. *Hydrol. Earth Syst. Sci.* 16, 3383–3390. <http://dx.doi.org/10.5194/hess-16-3383-2012>.
- Hänggi, P., Weingartner, R., Balmer, M., 2011. Auswirkungen der Klimaänderung auf die Wasserkraftnutzung in der Schweiz 2021–2050 – Hochrechnung. *Wasser Energ. Luft* 4, 300–307.
- Hall, D.K., Riggs, G.A., Salomonson V., DiGirolamo, N.E., Bayr, K.J., 2002. MODIS snow-cover products. *Remote Sens. Environ.* 83, 181–194. [http://dx.doi.org/10.1016/S0034-4257\(02\)00095-0](http://dx.doi.org/10.1016/S0034-4257(02)00095-0).
- Hantel, M., Hirtl-Wielke, L.-M., 2007. Sensitivity of Alpine snow cover to European temperature. *Int. J. Climatol.* 27, 1265–1275. <http://dx.doi.org/10.1002/joc.1472>.
- Horton, P., Schaeffli, B., Mezghani, A., Hingray, B., Musy, A., 2006. Assessment of climate-change impacts on alpine discharge regimes with climate model uncertainty. *Hydrol. Process.* 20, 2091–2109. <http://dx.doi.org/10.1002/hyp.6197>.
- Huss, M., Farinotti, D., 2012. Distributed ice thickness and volume of all glaciers around the globe. *J. Geophys. Res.* 117, 10. <http://dx.doi.org/10.1029/2012JF002523>.
- Huss, M., Fischer, M., 2016. Sensitivity of very small glaciers in the Swiss Alps to future climate change. *Front. Earth Sci.* 4. <http://dx.doi.org/10.3389/feart.2016.00034>.
- Huss, M., Farinotti, D., Bauder, A., Funk, M., 2008. Modelling runoff from highly glacierized alpine drainage basins in a changing climate. *Hydrol. Process.* 22, 3888–3902. <http://dx.doi.org/10.1002/hyp.7055>.
- Huss, M., Jouvett, G., Farinotti, D., Bauder, A., 2010. Future high-mountain hydrology: a new parameterization of glacier retreat. *Hydrol. Earth Syst. Sci.* 14, 815–829. <http://dx.doi.org/10.5194/hess-14-815-2010>.
- Huss, M., 2010. Mass balance of Pizolgletscher. *Geogr. Helv.* 65, 80–92.
- IPCC, 2014. *Climate change 2014: synthesis report. contribution of working groups I, II and III to the fifth assessment report of the intergovernmental panel on climate change*. In: Pachauri, R.K., Meyer, L.A., Core Writing Team, Russian Federation (Eds.), Hoelsing Lee (Republic of Korea) Scott B. Power (Australia) N.H. Ravindranath (India). IPCC, Geneva, Switzerland.
- Immerzeel, W.W., van Beek, L.P.H., Konz, M., Shrestha, A.B., Bierkens, M.F.P., 2012. Hydrological response to climate change in a glacierized catchment in the Himalayas. *Clim. Change* 110, 721–736. <http://dx.doi.org/10.1007/s10584-011-0143-4>.
- Johnston, P.R., Pilgrim, D.H., 1976. Parameter optimization for watershed models. *Water Resour. Res.* 12, 477–486. <http://dx.doi.org/10.1029/wr012i003p00477>.

- Jonas, T., Marty, C., Magnusson, J., 2009. Estimating the snow water equivalent from snow depth measurements in the Swiss Alps. *J. Hydrol.* 378, 161–167. <http://dx.doi.org/10.1016/j.jhydrol.2009.09.021>.
- Juston, J., Seibert, J., Johansson, P., 2009. Temporal sampling strategies and uncertainty in calibrating a conceptual hydrological model for a small boreal catchment. *Hydrol. Process.* 23, 3093–3109. <http://dx.doi.org/10.1002/hyp.7421>.
- Köplin, N., Schädler, B., Viviroli, D., Weingartner, R., 2013. The importance of glacier and forest change in hydrological climate-impact studies. *Hydrol. Earth Syst. Sci.* 17, 619–635. <http://dx.doi.org/10.5194/hess-17-619-2013>.
- Kirchner, J.W., 2006. Getting the right answers for the right reasons: linking measurements, analyses, and models to advance the science of hydrology. *Water Resour. Res.* 42. <http://dx.doi.org/10.1029/2005wr004362>.
- Knutti, R., Masson, D., Gattelman, A., 2013. Climate model genealogy: generation CMIP5 and how we got there. *Geophys. Res. Lett.* 40, 1194–1199. <http://dx.doi.org/10.1002/grl.50256>.
- Koboltschnig, G.R., Sch, W., Zappa, M., Kroisleitner, C., Holzmann, H., 2008. Runoff modelling of the glacierized Alpine Upper Salzach basin (Austria): multi-criteria result validation. *Hydrol. Processes* 22, 3950–3964. <http://dx.doi.org/10.1002/hyp.7112>.
- Kopytkovskiy, M., Geza, M., McCray, J.E., 2015. Climate-change impacts on water resources and hydropower potential in the Upper Colorado River Basin. *J. Hydrol. Reg. Stud.* 3, 473–493. <http://dx.doi.org/10.1016/j.ejrh.2015.02.014>.
- Kuczera, G., Mroczkowski, M., 1998. Assessment of hydrologic parameter uncertainty and the worth of multiresponse data. *Water Resour. Res.* 34, 1481–1489. <http://dx.doi.org/10.1029/98WR00496>.
- Latenser, M., Schneebeli, M., 2003. Long-term snow climate trends of the Swiss Alps (1931–99). *Int. J. Climatol.* 23, 733–750. <http://dx.doi.org/10.1002/joc.912>.
- Lehner, B., Czisch, G., Vassolo, S., 2005. The impact of global change on the hydropower potential of Europe: a model-based analysis. *Energy Policy* 33, 839–855. <http://dx.doi.org/10.1016/j.enpol.2003.10.018>.
- Li, H., Beldring, S., Xu, C.-Y., Huss, M., Melvold, K., Jain, S.K., 2015. Integrating a glacier retreat model into a hydrological model – case studies of three glacierised catchments in Norway and Himalayan region. *J. Hydrol.* 527, 656–667. <http://dx.doi.org/10.1016/j.jhydrol.2015.05.017>.
- Lichty, R.W., Dawdy, D.R., Bergmann, J.M., 1968. Rainfall-runoff model for small basin flood hydrograph simulation. *Use Analog Digit. Comput. Hydrol.* 81, 356–367.
- Lutz, A.F., Immerzeel, W.W., Shrestha, A.B., Bierkens, M.F.P., 2014. Consistent increase in High Asia's runoff due to increasing glacier melt and precipitation. *Nat. Clim. Chang.* 4, 587–592. <http://dx.doi.org/10.1038/nclimate2237>.
- Magnusson, J., Farinotti, D., Jonas, T., Bavay, M., 2010. Quantitative evaluation of different hydrological modelling approaches in a partly glacierized Swiss watershed. *Hydrol. Process.* 25, 2071–2084.
- McGuinness, J., Bordne, E., 1972. A Comparison of Lysimeter-Derived Potential Evapotranspiration with Computed Values.
- Metropolis, N., Ulam, S., 1949. The Monte Carlo method. *J. Am. Stat. Assoc.* 44, 335. <http://dx.doi.org/10.2307/2280232>.
- Mohor, G.S., Rodriguez, D.A., Tomasella, J., Siqueira Júnior, J.L., 2015. Exploratory analyses for the assessment of climate change impacts on the energy production in an Amazon run-of-river hydropower plant. *J. Hydrol. Reg. Stud.* 4, 41–59. <http://dx.doi.org/10.1016/j.ejrh.2015.04.003>.
- Mote, P.W., 2006. Climate-driven variability and trends in mountain snowpack in western North America. *J. Clim.* 19, 6209–6220. <http://dx.doi.org/10.1175/JCLI3971.1>.
- Motovilov, Y.G., Gottschalk, L., Engeland, K., Rodhe, A., 1999. Validation of a distributed hydrological model against spatial observations. *Agric. For. Meteorol.* 98–99, 257–277. [http://dx.doi.org/10.1016/S0168-1923\(99\)00102-1](http://dx.doi.org/10.1016/S0168-1923(99)00102-1).
- Muerth, M.J., Gauvin St-Denis, B., Ricard, S., Velázquez, J.A., Schmid, J., Minville, M., Caya, D., Chaumont, D., Ludwig, R., Turcotte, R., 2013. On the need for bias correction in regional climate scenarios to assess climate change impacts on river runoff. *Hydrol. Earth Syst. Sci.* 17, 1189–1204. <http://dx.doi.org/10.5194/hess-17-1189-2013>.
- Nash, J.E., Sutcliffe, J.V., 1970. River flow forecasting through conceptual models, part 1—a discussion of principles. *J. Hydrol.* 10, 282–290.
- Nohara, D., Kitoh, A., Hosaka, M., Oki, T., 2006. Impact of climate change on river discharge projected by multimodel ensemble. *J. Hydrometeorol.* 7, 1076–1089. <http://dx.doi.org/10.1175/JHM531.1>.
- Panofsky, H.W., Brier, G.W., 1968. *Some Applications of Statistics to Meteorology*. The Pennsylvania State University Press, Philadelphia.
- Paul, F., Kääb, A., Haeblerli, W., 2007. Recent glacier changes in the Alps observed by satellite: consequences for future monitoring strategies. *Glob. Planet. Change* 56, 111–122. <http://dx.doi.org/10.1016/j.gloplacha.2006.07.007>.
- Paul, F., Escher-Vetter, H., Machguth, H., 2009. Comparison of mass balances for Vernagtferner, Oetzal Alps, as obtained from direct measurements and distributed modeling. *Ann. Glaciol.* 50, 169–177. <http://dx.doi.org/10.3189/172756409787769582>.
- Piani, C., Weedon, G.P., Best, M., Gomes, S.M., Viterbo, P., Hagemann, S., Haerter, J.O., 2010. Statistical bias correction of global simulated daily precipitation and temperature for the application of hydrological models. *J. Hydrol.* 395, 199–215. <http://dx.doi.org/10.1016/j.jhydrol.2010.10.024>.
- Rasmus, S., Räisänen, J., Lehning, M., 2004. Estimating snow conditions in Finland in the late 21st century using the SNOWPACK model with regional climate scenario data as input. *Ann. Glaciol.* 38, 238–244. <http://dx.doi.org/10.3189/17275640781814843>.
- Ravazzani, G., Dalla Valle, F., Gaudard, L., Mendlik, T., Gobiet, A., Mancini, M., 2016. Assessing climate impacts on hydropower production: the case of the toce river basin. *Climate* 4, 16. <http://dx.doi.org/10.3390/cli4020016>.
- SGHL, CHy, 2011. Auswirkungen der Klimaänderung auf die Wasserkraftnutzung – Synthesebericht. Published by Swiss Society for Hydrology and Limnology (SGHL) and the Swiss Hydrological Commission (CHy). Beiträge zur Hydrol. der Schweiz 38.
- Schaeffli, B., Hingray, B., Musy, A., 2007. Climate change and hydropower production in the Swiss Alps: quantification of potential impacts and related modelling uncertainties. *Methodology: Overview* 11, 1191–1205.
- Schwarb, M., 2000. *The Alpine Precipitation Climate: Evaluation of a High-Resolution Analysis Scheme Using Comprehensive Rain-Gauge Data*. Swiss Federal Institute of Technology, Zurich.
- Seibert, J., Beven, K., 2009. Gauging the ungauged basin: how many discharge measurements are needed? *Hydrol. Earth Syst. Sci.* 13, 883–892. <http://dx.doi.org/10.5194/hess-13-883-2009>.
- Seibert, J., Vis, M.J.P., 2012. Teaching hydrological modeling with a user-friendly catchment-runoff-model software package. *Hydrol. Earth Syst. Sci.* 16, 3315–3325. <http://dx.doi.org/10.5194/hess-16-3315-2012>.
- Seibert, J., Vis, M.J.P., Kohn, I., Weiler, M., Stahl, K., 2017. Technical Note: Representing glacier dynamics in a semi-distributed hydrological model. *Hydrol. Earth Syst. Sci.* <http://dx.doi.org/10.5194/hess-2017-158>.
- Sheffield, J., Wood, E.F., Roderick, M.L., 2012. Little change in global drought over the past 60 years. *Nature* 491, 435–438. <http://dx.doi.org/10.1038/nature11575>.
- Stahl, K., Moore, R.D., Shea, J.M., Hutchinson, D., Cannon, A.J., 2008. Coupled modelling of glacier and streamflow response to future climate scenarios. *Water Resour. Res.* 44. <http://dx.doi.org/10.1029/2007WR005956>.
- Swiss Federal Office for the Environment, 2012. Auswirkungen der Klimaänderung auf Wasserressourcen und Gewässer. Synthesebericht zum Projekt «Klimaänderung und Hydrologie in der Schweiz» (CCHydro). Umwelt-Wissen Nr. 1217, Bundesamt für Umwelt, Bern.
- Terzago, S., von Hardenberg, J., Palazzi, E., Provenzale, A., 2017. Snow water equivalent in the Alps as seen by gridded datasets, CMIP5 and CORDEX climate models. *Cryosph. Discuss.* 1–30. <http://dx.doi.org/10.5194/tc-2016-280>.
- Teutschbein, C., Seibert, J., 2012. Bias correction of regional climate model simulations for hydrological climate-change impact studies: review and evaluation of different methods. *J. Hydrol.* 456–457, 12–29. <http://dx.doi.org/10.1016/j.jhydrol.2012.05.052>.
- Themessl, M.J., Gobiet, A., Leuprecht, A., 2011. Empirical-statistical downscaling and error correction of daily precipitation from regional climate models. *Int. J. Climatol.* 31, 1530–1544. <http://dx.doi.org/10.1002/joc.2168>.
- Tobin, I., Vautard, R., Balog, I., Bréon, F.-M., Jerez, S., Ruti, P.M., Thais, F., Vrac, M., Yiou, P., 2015. Assessing climate change impacts on European wind energy from ENSEMBLES high-resolution climate projections. *Clim. Change* 128, 99–112. <http://dx.doi.org/10.1007/s10584-014-1291-0>.
- Uhlenbrook, S., Sieber, A., 2005. On the value of experimental data to reduce the prediction uncertainty of a process-oriented catchment model. *Environ. Model. Softw.* 20, 19–32. <http://dx.doi.org/10.1016/j.envsoft.2003.12.006>.
- van Vliet, M.T.H., Wiberg, D., Leduc, S., Riahi, K., 2016. Power-generation system vulnerability and adaptation to changes in climate and water resources. *Nat. Clim. Chang.* 6, 375–380. <http://dx.doi.org/10.1038/nclimate2903>.

- van der Linden, P., Mitchell, J.F.B., 2009. *Climate Change and Its Impacts: Summary of Research and Results from the ENSEMBLES Project*. FitzRoy Road, Exeter EX1 3PB.
- von Storch, H., Zwiers, F.W., 1999. *Statistical Analysis in Climate Research*. Cambridge University Press.
- Vetter, T., Reinhardt, J., Flörke, M., van Griensven, A., Hattermann, F., Huang, S., Koch, H., Pechlivanidis, I.G., Plötner, S., Seidou, O., Su, B., Vervoort, R.W., Kryanova, V., 2017. Evaluation of sources of uncertainty in projected hydrological changes under climate change in 12 large-scale river basins. *Clim. Change* 141, 419–433. <http://dx.doi.org/10.1007/s10584-016-1794-y>.
- Vormoor, K., Lawrence, D., Heistermann, M., Bronstert, A., 2015. Climate change impacts on the seasonality and generation processes of floods—projections and uncertainties for catchments with mixed snowmelt/rainfall regimes. *Hydrol. Earth Syst. Sci.* 19, 913–931. <http://dx.doi.org/10.5194/hess-19-913-2015>.
- Zemp, M., Frey, H., Gärtner-Roer, I., Nussbaumer, S.U., Hoelzle, M., Paul, F., Haeberli, W., Denzinger, F., Ahlstrøm, A.P., Anderson, B., Bajracharya, S., Baroni, C., Braun, L.N., Cáceres, B.E., Casassa, G., Cobos, G., Dávila, L.R., Delgado Granados, H., Demuth, M.N., Espizua, L., Fischer, A., Fujita, K., Gadek, B., Ghazanfar, A., Hagen, J.O., Holmlund, P., Karimi, N., Li, Z., Pelto, M., Pitte, P., Popovnin, V.V., Portocarrero, C.A., Prinz, R., Sangewar, C.V., Severskiy, I., Sigurdsson, O., Soruco, A., Usabaliev, R., Vincent, C., 2015. Historically unprecedented global glacier decline in the early 21st century. *J. Glaciol.* 61, 745–762. <http://dx.doi.org/10.3189/2015JoG15J017>.
- Zierl, B., Bugmann, H., 2005. Global change impacts on hydrological processes in Alpine catchments. *Water Resour. Res.* 41, 1–13. <http://dx.doi.org/10.1029/2004WR003447>.